How to hit home runs: Optimum baseball bat swing parameters for maximum range trajectories

Gregory S. Sawicki and Mont Hubbard[a)]
Department of Mechanical and Aeronautical Engineering, University of California, One Shields Avenue, Davis, California 95616

William J. Stronge
Department of Engineering, University of Cambridge, Cambridge CB2 1PZ, United Kingdom

(Received 12 June 2002; accepted 3 July 2003)

Improved models for the pitch, batting, and post-impact flight phases of a baseball are used in an optimal control context to find bat swing parameters that produce maximum range. The improved batted flight model incorporates experimental lift and drag profiles (including the drag crisis). An improved model for bat–ball impact includes the dependence of the coefficient of restitution on the approach relative velocity and the dependence of the incoming pitched ball angle on speed. The undercut distance and bat swing angle are chosen to maximize the range of the batted ball. The sensitivity of the maximum range is calculated for all model parameters including bat and ball speed, bat and ball spin, and wind speed. Post-impact conditions are found to be independent of the ball–bat coefficient of friction. The lift is enhanced by backspin produced by undercutting the ball during batting. An optimally hit curve ball will travel farther than an optimally hit fastball or knuckleball due to increased lift during flight. © *2003 American Association of Physics Teachers.*
[DOI: 10.1119/1.1604384]

I. INTRODUCTION

In baseball, the home run is a sure way to score and the problem of hitting the ball as far as possible is as old as the game. An analysis of the problem consists of two phases: impact and flight. Many previous investigations have considered one or both of the phases of this problem. Briggs[1] investigated the effects of velocity and spin on the lateral deflection of a curve ball. Baseballs spinning about a vertical axis were dropped through a horizontal wind tunnel. The lateral deflection of the ball was found to be proportional to the spin and the square of the translational velocity for speeds up to 150 ft/s and spins up to 1800 rpm. Achenbach[2] characterized the drag on spheres as a function of the Reynolds number Re and the surface roughness. He showed that there is a critical Reynolds number at which the drag coefficient C_D decreases dramatically and that this critical Reynolds number decreases as the roughness increases. Although a baseball is not uniformly rough, the spinning seams cause boundary layer behavior similar to that of a rough surface.

Based on the results of Ref. 1, the knuckleball was investigated by Watts and Sawyer.[3] They used a wind tunnel to determine that the lift depends on the seam orientation in relation to the relative wind velocity. They found that an oscillating lateral force can result from a portion of the seam being located just at the point where boundary layer separation occurs. Frohlich[4] was the first to point out that there is a strong possibility that the drag crisis, a sharp reduction in the drag coefficient at the critical Reynolds number, occurs at speeds typical of pitched or batted baseballs. He stated that, "The effects of drag reduction on the behavior of both pitched and batted balls is significant ... the drag reduction may help to explain why pitched fastballs appear to rise, why pitched curve balls appear to drop sharply, and why home run production has increased since the introduction of the alleged 'lively ball.'" Frohlich emphasized that the coefficient of drag must be considered to be a function of Re (and hence the velocity) in an accurate and realistic simulation of baseball flight. He noted that the fastest pitchers in the major leagues (45 m/s) produce values of Re well beyond the drag crisis for roughened spheres and suggested that, "If a batter desiring a home run can hit a ball hard enough to 'punch through' the drag crisis, he can hit the ball considerably farther than would be expected if the drag coefficient were constant."

Rex[5] studied the effect of spin on the flight of batted baseballs and found that balls hit with backspin tend to travel farther than balls hit with little spin or topspin. He assumed a constant C_D of 0.5 and a Magnus force coefficient taken from the earlier work of Briggs,[1] and suggested that the effect of backspin on increasing range is enhanced as the initial angle of the ball flight trajectory is decreased. Watts and Ferrer[6] measured the lateral forces on a spinning baseball in a wind tunnel and concluded that the lift coefficient C_L is a function of the spin parameter $S=r\omega/v$, where r, ω, and v are the ball radius, spin and speed, respectively, and at most a weak function of Re. Watts and Baroni[7] calculated the trajectories of batted baseballs in a vertical plane using $C_D=0.5$ and C_L based on the data of Ref. 6. Their results agreed with those of Ref. 5 in that range increased with backspin (seemingly without bound) and that as the spin increased, the optimum launch angle decreased.

Alaways *et al.*[8] matched a dynamic model of baseball flight with experimental data to identify the release conditions and aerodynamic forces on pitched baseballs; C_D was considered constant over the trajectory of a single pitch, but generally differed between pitches. The estimated C_D (which showed a minimum at Re~165 000) agreed well with the previously reported data in Ref. 2 and supported the suggestion[4] that the drag crisis may affect pitched baseballs.

Alaways and Hubbard[9] developed a method for determining the lift on spinning baseballs, again matching experimental pitch data. Their results bridged the gap in the C_L data of Ref. 6 at low values of the spin parameter. In addition, their results correlated well with previous data and showed that

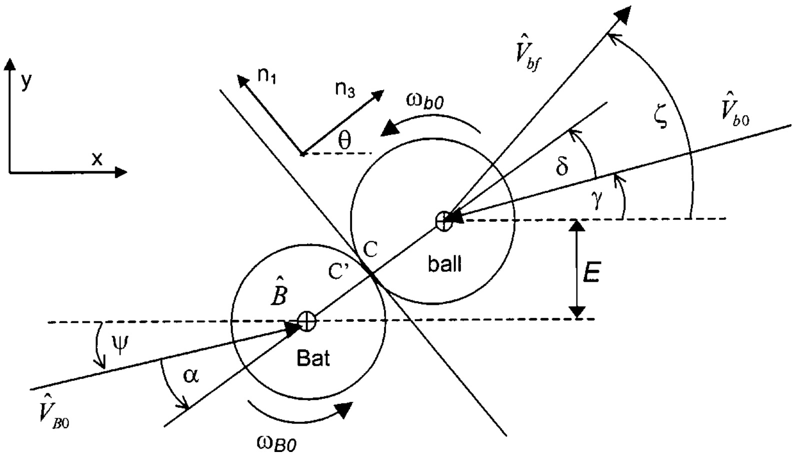

Fig. 1. Two-dimensional impact schematic. The bat–ball contact occurs with the bat horizontal, but with both vertical and horizontal components of bat and ball velocities and bat and ball spin. The batted ball speed $\hat{V}_{bf}$, launch angle ζ, and spin ω_{bf} are functions of pre-impact bat and ball speed and spin, the angle γ, and the two primary batter controlled parameters, E and ψ.

the seam orientation has a stronger effect on C_L than Re when the spin is small. As the spin parameter increases, the influence of seam orientation decreases.

The impact problem also has been studied. Kirkpatrick[10] analyzed the collision between the bat and ball assuming that the bat is swung in a horizontal plane. Kagan[11] did an analytical calculation of the sensitivity of the range to the coefficient of restitution. Other authors have considered the bat–ball impact, but mostly from the point of view of bat vibration and the location of a sweet spot.[12–16]

In addition to the effect of backspin on the trajectory of a baseball, the backspin that results from oblique impact with friction between the bat and ball has been calculated.[7] Classical rigid body collision theory was used to show that if the coefficient of friction is not too small, the batter can generate large backspin by undercutting the ball center by as much as 1–2.5 cm, although the coefficient of friction that they employed (μ=0.05–0.1) is too small to be considered representative of collisions between bat and ball. Watts and Baroni[7] were the first to suggest that an optimum batting strategy might exist, namely that there might be an optimum combination of ball backspin and launch angle for a given initial batted ball speed.

Although the optimal initial flight conditions were considered in Ref. 7, the authors did not explicitly present the manner in which the batter could produce them. In this paper we combine improved models of both the impact and flight with optimization techniques that allow the direct calculation of the optimum bat swing parameters (rather than initial flight parameters), undercut distance, and bat swing plane angle for different pitches. We also present the sensitivities of the optimal solutions to other relevant parameters and environmental factors.

II. METHODS AND CALCULATIONS

A. Initial conditions for impact

Figure 1 shows the kinematic properties of the bat (left) and the ball (right) at the instant of collision. These properties are expressed in an impact reference frame $\mathbf{n}_i$ oriented relative to the common tangent plane passing through the coincident contact points C and C' on the ball and bat, respectively. Contact is assumed to occur with the bat horizontal and perpendicular to the assumed vertical plane of flight of the pitched (and batted) ball. The orthonormal impact coordinate frame contains a unit vector $\mathbf{n}_3$ normal to the common tangent plane, another unit vector $\mathbf{n}_1$ in the common tangent plane, and a unit vector $\mathbf{n}_2=\mathbf{n}_3\times\mathbf{n}_1$ that is normal to the vertical plane of flight (see Fig. 1). Initial conditions for the impact depend on the type and speed of the pitch as well as the bat velocity and positioning relative to the ball.

The ball velocities are initially defined in an inertial orthogonal (flight) frame with positive x toward center field, positive y skyward, and positive z from the pitchers mound toward first base. The angles between the horizontal and the incident ball velocity vector $\hat{\mathbf{V}}_{b0}$ and between the ball velocity vector and the common normal $\mathbf{n}_3$, are termed γ and δ, respectively, and are both positive counterclockwise (Fig. 1). The symbol ˆ denotes the location in the flight plane of the projection of the center of mass for a body. Subscripts b, B, 0, f, and p denote ball, bat, pre-impact, post-impact, and pitcher, respectively. Likewise, the bat has incident velocity magnitude $\hat{V}_B$ at the point $\hat{B}$ on its axis in the $\mathbf{n}_1-\mathbf{n}_3$ plane. The angle between the horizontal and the bat initial velocity vector is ψ, and α denotes the angle between the bat velocity vector and the common normal $\mathbf{n}_3$, again both positive counterclockwise. The angle θ between the horizontal and $\mathbf{n}_3$ is related to the undercut distance (defined as the difference in y coordinates of the ball and bat and positive when the bat axis is below the ball center; see Fig. 1) by

$$\theta=\sin^{-1}\left(\frac{E}{r_b+r_B}\right). \tag{1}$$

The other angles satisfy the relations

$$\delta=\theta-\gamma, \quad \alpha=\theta-\psi. \tag{2}$$

The angle γ is a function of the pitch speed at the plate, $\hat{V}_{b0}$. A faster pitched ball that crosses the plate in the strike zone has a relatively larger downward vertical velocity component, both when pitched, $\hat{V}_{byp}$, and at the plate, $\hat{V}_{by0}$. If we fit the data in Fig. 6 of Ref. 8, $\hat{V}_{byp}$ varies with pitch speed $\hat{V}_{bp}$ roughly according to $\hat{V}_{byp}=-(\hat{V}_{bp}-36)/3.4$ in m/s. We used the approximations that $\hat{V}_{by0}=\hat{V}_{byp}-gt$, where g is the acceleration due to gravity and t is the flight time, $t=D/\hat{V}_{bp}$, where $D=18.52$ m is the distance from the mound to home plate. We have used the fact that a typical pitch loses about 5% of its speed during the pitch $\hat{V}_{b0}=0.95\,\hat{V}_{bp}$ (from Fig. 6 of Ref. 8). We then estimate the final vertical speed of the ball at the plate given the magnitude of the ball velocity at the plate

Table I. Model parameters and variables. The subscripts b and B refer to ball and bat, respectively; the subscripts 0, f, and p refer to pre-impact, post-impact, and pitch release, respectively; subscripts 1, 2, 3 and x, y, z refer to the components of vectors in the orthonormal impact and inertial reference frames, respectively.

Symbol	Description	Value
g	Gravitational acceleration constant	9.81 m/s^2
ρ	Atmospheric density	1.23 kg/m^3
μ	Static coefficient of friction	0.50±0.04 wood 0.35±0.03 aluminum
ν	Kinematic viscosity of air	$1.5e^{-5}$ m^2/s
C_D	Drag coefficient	
C_L	Lift coefficient	
M_b	Baseball mass	0.145 kg (5.1 oz)
M'_B	Bat mass	0.9 kg (31.7 oz)
r_b	Baseball radius	0.0366 m (1.44 in.)
r_B	Bat barrel radius	0.0350 m (1.38 in.)
k_{B1}	Radius of gyration of bat for c.m. about $\mathbf{n}_1$ axis	0.217 m (8.54 in.)
k_{B2}	Radius of gyration of bat about $\mathbf{n}_2$ axis	0.0231 m (0.91 in.)
k_b	Radius of gyration of ball about c.m.	0.0247 m (0.97 in.)
E	Undercut distance	
θ	Angle of common normal $\mathbf{n}_3$ from horizontal	
α	Bat swing angle from common normal	
ψ	Bat swing angle from horizontal	
γ	Pitched ball velocity angle from horizontal	
δ	Pitched ball velocity angle from common normal	
$\hat{V}_{b0}$	Pitched ball speed at plate	
$\hat{V}_{B0}$	Pre-impact bat speed at $\hat{B}$	
ω_{b0}	Pre-impact ball spin magnitude	
ω_{B0}	Pre-impact bat spin magnitude	
ω_{bf}	Post-impact ball angular velocity	
$\mathbf{V}_w$	Wind velocity	
$\hat{\mathbf{V}}_{bf}$	Post-impact ball c.m. velocity	
$\mathbf{V}_{bf}$	Post-impact ball velocity at contact point	
$\mathbf{V}_{Bf}$	Post-impact bat velocity at contact point	
ζ	Post-impact ball velocity angle from horizontal	

$$\hat{V}_{by0}=\frac{-\hat{V}_{b0}^2+36\times 0.95\times\hat{V}_{b0}-3.42\times 0.95^2\times g\times 18.52}{3.42\times 0.95\times\hat{V}_{b0}}$$
$$=\frac{-\hat{V}_{b0}^2+34.2\times\hat{V}_{b0}-561}{3.25\times\hat{V}_{b0}}. \tag{3}$$

The angle γ can be expressed as

$$\gamma=-\sin^{-1}\left(\frac{\hat{V}_{by0}}{\hat{V}_{b0}}\right). \tag{4}$$

The ball has mass M_b, radius r_b, angular velocity magnitude ω_b and center of mass (c.m.) velocity magnitude $\hat{V}_b$; the bat has mass M'_B, barrel radius r_B, and angular velocity ω_B about its axis (Table I). The bat has a radius of gyration about its axis k_{B2} and the ball's radius of gyration about its center is k_b.

We further assume that the ball strikes the bat along its length at the center of percussion relative to the handle end; this point is located about 83 mm outside the center of mass.[17] This assumption ensures that, as the ball strikes the bat, there will be no impulsive reaction between the handle and the batter's hands. Furthermore, because this point is near the nodes of the first and second free vibration modes, vibrational energy loss is minimized and a rigid body model for the bat is a good approximation.[16] With the impact point at some distance from the center of mass however, the effective inertia of the bat at the impact point is reduced. For a bat of actual mass $M'_B=0.9\,\mathrm{kg}\,(32\,\mathrm{oz})$, a radius of gyration about a transverse axis through the center of mass,[17] $k_{B1}=0.217\,\mathrm{m}$, and impact at the center of percussion, the present two-dimensional analysis gives an equivalent bat mass $M_B=0.8\,\mathrm{kg}$ to have the same impulse for the period of compression. This equivalent mass for the planar (two-dimensional) impact analysis is calculated from $M_B/M'_B=(1+z^2/k_{B1}^2)^{-1}$, where $z=z_{cp}-z_{\mathrm{c.m.}}$ is the axial distance of the impact point from the bat center of mass.

B. Impact analysis

The analysis of the oblique impact of rough, hard bodies follows the planar rigid-body impact methodology and terminology developed by Stronge.[18] This approach is more complex than that used in Ref. 7 and is chosen to provide a formalism that can be used in potentially more complex batting geometries in which the bat is not constrained to remain horizontal and the ball and bat can have other than horizontal components of spin and lateral components of velocity. The formalism expresses the changes in relative velocity at the contact point as a function of the normal component impulse and hence calculates the bat and ball conditions at separation. Although significant ball deformations can occur during batting, this analysis assumes rigid-body impact where the inertia properties are invariant and contact duration is negligibly small as a consequence of deflections being small.

In the impact reference frame and using indicial notation, the position vectors to the contact point C from the center of mass of the ball r_{bi} and from the point $\hat{B}$ on the bat axis $r_{\hat{B}i}$ are expressed as, respectively,

$$r_{bi}=\begin{pmatrix}0\\0\\-r_b\end{pmatrix},\quad r_{Bi}=\begin{pmatrix}0\\0\\r_B\end{pmatrix}. \tag{5}$$

At the contact point of each body, a reaction force F_{Bi} or F_{bi} develops that opposes the interpenetration of the bodies during impact. These forces are related to differentials of the impulse dP_{Bi} and dP_{bi} at C and C' by

$$dP_{Bi}=F_{Bi}dt,\quad dP_{bi}=F_{bi}dt\quad (i=1,3), \tag{6}$$

where the subscripts 1 and 3 denote the tangential and normal components of the vectors. Because the present model is two-dimensional, the components along the two axis are identically zero. Newton's equations of motion for translation of the center of mass of the ball and point $\hat{B}$ of the bat are

$$\begin{aligned}d\hat{V}_{bi}&=M_b^{-1}dP_{bi},\\ d\hat{V}_{Bi}&=M_B^{-1}dP_{Bi},\end{aligned}\quad i=1,3 \tag{7}$$

and the differential rotation of each rigid body about n_2 is described by

$$\begin{aligned}d\omega_{bi}&=(M_bk_b^2)^{-1}r_{bi}\times dP_{bi},\\ d\omega_{Bi}&=(M_Bk_{B2}^2)^{-1}r_{Bi}\times dP_{Bi}.\end{aligned} \tag{8}$$

Using the construct of an infinitesimal deformable particle between the points of contact,[18] the changes in the relative velocity between the bodies at the contact point C are obtained as a function of impulse $P_i(i=1,3)$ during the contact. In order to handle distinct periods of slip or stick during impact, the period of collision can be characterized as a function of a continuous independent variable, the impulse P_i.

The velocity of the contact point on each rigid body, $V_{bi}(P_{bi})$ or $V_{Bi}(P_{Bi})$, is a function of the reaction impulse and is related to the velocity of the corresponding center through

$$\begin{aligned}V_{bi}&=\hat{V}_{bi}+(\omega_{bi}\times r_{bi}),\\ V_{Bi}&=\hat{V}_{Bi}+(\omega_{Bi}\times r_{Bi}).\end{aligned} \tag{9}$$

The relative velocity across the contact point is the velocity difference

$$v_i=V_{bi}-V_{Bi}, \tag{10}$$

and the effective mass m is defined as

$$m=\frac{M_bM_B}{M_b+M_B}. \tag{11}$$

We note that the contact forces acting on each body are equal and opposite, $dp_i=dP_{bi}=-dP_{Bi}$. If we substitute Eqs. (7)–(9) into Eq. (10), the differential equations of motion can be written in matrix form. If we express the differential of the relative velocity at the contact point as a function of the differential impulse, we obtain

$$\begin{Bmatrix}dv_1\\dv_3\end{Bmatrix}=m^{-1}\begin{bmatrix}\beta_1&-\beta_2\\-\beta_2&\beta_3\end{bmatrix}\begin{Bmatrix}dp_1\\dp_3\end{Bmatrix}, \tag{12}$$

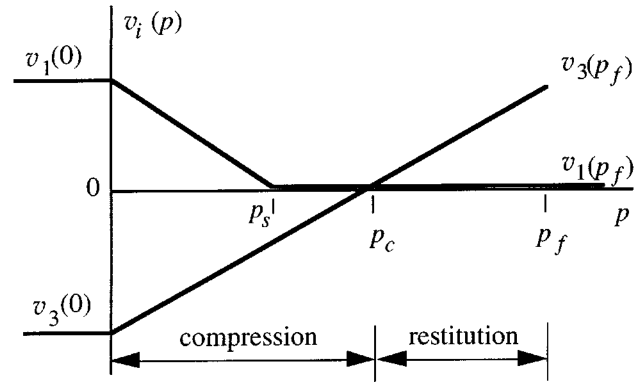

Fig. 2. Changes in components of relative velocity with normal impulse p during collinear impact with slip-stick at the contact point C.

where the elements of the inverse of the inertia matrix can be expressed as

$$\begin{aligned}\beta_1&=1+\frac{mr_{b3}^2}{M_bk_b^2}+\frac{mr_{B3}^2}{M_Bk_{B2}^2},\\ \beta_2&=\frac{mr_{b1}r_{b3}}{M_bk_b^2}+\frac{mr_{B1}r_{B3}}{M_Bk_{B2}^2},\\ \beta_3&=1+\frac{mr_{b1}^2}{M_bk_b^2}+\frac{mr_{B1}^2}{M_Bk_{B2}^2}.\end{aligned} \tag{13}$$

Finally, the tangential and normal components of differential impulse can be related using the Amonton–Coulomb law[18] for dry friction:

$$dp_1=-\mu s\,dp_3,\quad s=\begin{cases}1, & v_1(p_3)>0\\ 0, & v_1(p_3)=0\\ -1, & v_1(p_3)<0\end{cases}, \tag{14}$$

where s characterizes the direction of slip, and the static and dynamic coefficients of friction are denoted by μ and assumed to be equal. The negative sign in Eq. (14) ensures that friction opposes the direction of slip. The differential equations of motion for the impact can then be expressed in terms of a single independent variable, the normal reaction impulse $p_3\equiv p$:

$$\begin{aligned}dv_1&=m^{-1}(-\mu s\beta_1-\beta_2)dp,\\ dv_3&=m^{-1}(\mu s\beta_2+\beta_3)dp.\end{aligned} \tag{15}$$

At the contact point between bat and ball, the components of the initial relative velocity for impact are given by

$$\begin{aligned}v_1(0)&=\hat{V}_{b1}(0)+r_{b3}\omega_{b2}(0)-\hat{V}_{B1}(0)-r_{B3}\omega_{B2}(0),\\ v_3(0)&=\hat{V}_{b3}(0)-\hat{V}_{B3}(0).\end{aligned} \tag{16}$$

In the bat–ball collision $r_{B1}=r_{b1}=0$, and thus $\beta_2=0$ and $\beta_3=1$.

If we integrate Eq. (15) and set the relative velocity components to zero, we can calculate the normal impulse p_s required to bring the initial slip to a halt and the normal impulse p_c that makes the initial normal relative motion vanish (the impulse for compression as shown in Fig. 2):

$$p_s = \frac{m v_1(0)}{\mu s \beta_1}, \tag{17}$$

$$p_c = -m v_3(0). \tag{18}$$

When $p > p_s$, the tangential relative motion can either stick (pure rolling ensues) or slip in the opposite direction. In order for a collision with initial slip to stick after p_s a specific ratio of tangential to normal reaction force is required; this ratio is termed the coefficient for stick $\bar{\mu}$. For planar impact, $\bar{\mu} = \beta_2 / \beta_1$. For the bat–ball collision $\beta_2 = 0$, so that $\bar{\mu} = 0$; consequently if slip is brought to a halt, the contact will subsequently stick because $\mu > \bar{\mu}$.

Following the period of compression there is a period of restitution during which some normal relative motion is restored. Restitution ends at the final impulse p_f when separation occurs. In an elastic collision all of the energy is restored and the coefficient of energetic restitution $e_* = 1$. In an inelastic collision some energy is dissipated and $0 < e_* < 1$. It has been shown that e_* is a function of the relative velocity between the contact points (impact velocity) in the normal direction at the instant of impact. In general, e_* decreases with increasing normal initial relative velocity. We assume the relation between e_* and the normal relative velocity based on a linear fit to the data of Ref. 19, which coincides with the NCAA standard that at 60 mph, $0.525 < e_* < 0.550$:

$$e_* = 0.540 - \left(\frac{v_3(0) - 26.8}{400} \right), \tag{19}$$

where $v_3(0)$ is measured in m/s. The coefficient of restitution for aluminum bats is slightly higher than that for wood. The normal impulse at separation p_f can be written as

$$p_f = p_c (1 + e_*). \tag{20}$$

We are interested in the ball velocity and spin after bat impact, which depend on the final impulse p_f. If $p_s > p_f$, the contact slips throughout the impact period, and the final tangential impulse is limited by p_f. If $p_s < p_f$, slip halts during impact and the tangential impulse is limited by p_s; this occurs if the initial slip is small, $v_1(0)/v_3(0) < (1 + e_*) \times (\mu s \beta_1)$. We have

$$\begin{aligned} \mathbf{p}_f &= \begin{pmatrix} -\mu s p_s \\ 0 \\ p_f \end{pmatrix}, \quad p_s < p_f, \\ \mathbf{p}_f &= \begin{pmatrix} -\mu s p_f \\ 0 \\ p_f \end{pmatrix}, \quad p_s > p_f. \end{aligned} \tag{21}$$

Finally, by using the results from Eq. (20), we can express the state of the ball at separation from impact as:

$$\begin{aligned} \hat{\mathbf{V}}_b(p_f) &= \hat{\mathbf{V}}_b(0) - M_b^{-1} \mathbf{p}_f, \\ \boldsymbol{\omega}_b(p_f) &= \boldsymbol{\omega}_b(0) + \left(\frac{1}{M_b k_b^2} \right) \mathbf{r}_b \times \mathbf{p}_f, \end{aligned} \tag{22}$$

$$\zeta = \theta + \tan^{-1} \left(\frac{\hat{V}_{bf1}}{\hat{V}_{bf3}} \right). \tag{23}$$

The post-impact ball velocity and spin in Eq. (22) and launch angle in Eq. (23) define the initial conditions for simulation of the flight phase.

C. Friction measurement

The coefficient of friction μ between bat and ball was measured using a variant of the inclined plane experiment. Two new bats were taped together with the horizontal axes of their cylindrical barrels parallel. Two balls, also taped together to prevent rolling, were set in the groove formed by the bats' top surfaces, taking care to ensure that only the balls' leather surfaces contacted the bats. The knobs of the bats were slowly raised until slip occurred. A three-dimensional force balance at incipient slip shows that μ is given by

$$\mu = \tan \kappa \cos \sigma, \tag{24}$$

where κ is the angle of the long axes of the bats from the horizontal and σ is half the angle between the normal vectors to the two contact planes between a ball and the two bats. Because the static and kinetic coefficients of friction are not very different in general, and because the results presented below are relatively insensitive to μ, we assume that the static coefficient of friction determined in this way is representative of sliding as well.

D. Flight simulation

Given the post-impact ball velocity and spin [Eq. (22)] and launch angle [Eq. (23)], it is possible to calculate the trajectory in the $x-y$ plane (Fig. 1) and the resulting range. The spin of the ball in the flight phase follows the same sign convention as in the impact section; the batted ball backspin and pitched ball topspin are positive. The dominant gravity force $M_b g$ acts in the negative y direction. The aerodynamic drag force acts in the direction of the relative wind velocity

$$\mathbf{V}_r = \mathbf{V}_w - \mathbf{V}_b, \tag{25}$$

where $\mathbf{V}_b$ and $\mathbf{V}_w$ are the ball and wind velocity vectors, respectively. The drag force is given by

$$D = \frac{\rho A C_D |\mathbf{V}_r| \mathbf{V}_r}{2}, \tag{26}$$

where the frontal area $A = \pi r_b^2$ and ρ is the air density. C_D can be determined experimentally using wind tunnel or flight tests and is a strong function of Re, where

$$\mathrm{Re} = \frac{2 |\mathbf{V}_r| r_b}{\nu}, \tag{27}$$

where ν is the kinematic viscosity of air.

The drag coefficient C_D is also a function of the roughness of the ball surface. Although over a wide range of speeds (and hence Re), the drag coefficient for a sphere remains nearly constant at about $C_D = 0.5$, it was shown in Ref. 2 that an abrupt decrease by a factor of between 2 and 5 in drag (termed the "drag crisis") occurs at a value of Re in the range $0.6 \times 10^5 < \mathrm{Re} < 4.0 \times 10^5$, depending on the roughness of the surface. The work of both Refs. 2 and 4 makes it clear that to obtain accurate baseball trajectories, it is essential that the drag crisis be included in the model through the dependence of C_D on Re.

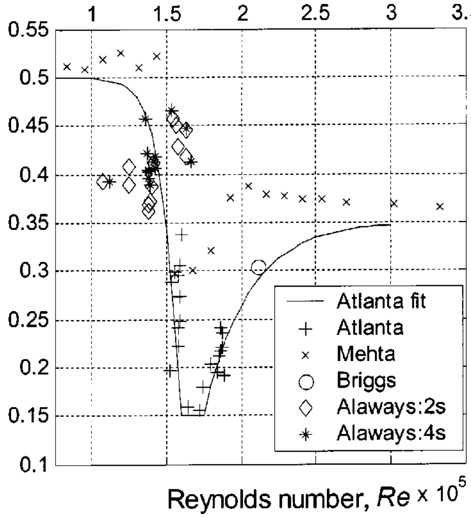

Fig. 3. Drag coefficient C_D vs Reynolds number Re. The drag decreases precipitously at Re 1.6×10^5 ($V\sim32$ m/s $=72$ mph) which strongly affects the batted range.

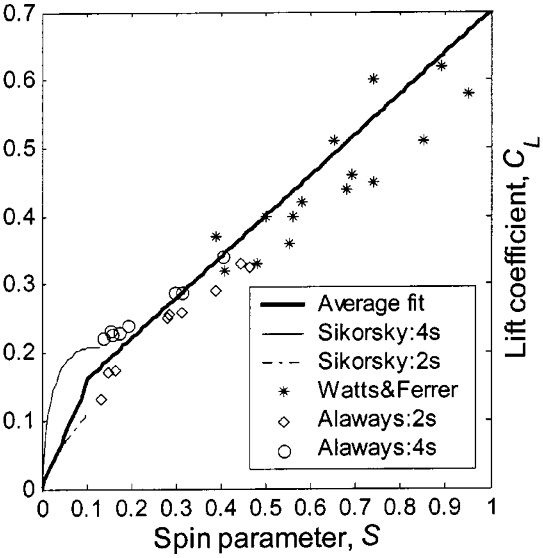

Fig. 4. Lift coefficient C_L vs spin parameter S. The large effect of ball spin orientation (two seam vs four seam pitches) at small S decreases as S increases.

In our model this dependence (Fig. 3) is taken from pitched baseball data collected at the 1996 Atlanta Olympics.[8] We fit two exponential functions to the data points, one below and one above the drag crisis, each rising from the minimum value for C_D (0.15) at values of Re near the drag crisis (~160 000 and 175 000). Also shown in Fig. 3 are baseball drag data from wind tunnel tests of nonspinning balls[20] in which a less severe drag crisis occurs at almost the same values of Re. Apparently the severity of the drag crisis is different for spinning and nonspinning balls. Briggs[1] has reported that, in an experiment by Dryden, a baseball was suspended in the air stream of a vertical wind tunnel with an airspeed about 42.7 m/s (Re $=208\,000$), which results in $C_D=0.3$ (plotted as ○ in Fig. 3). The measurements of Ref. 8 indicate that this point lies on a section of the drag curve where C_D is increasing (during recovery from the drag crisis), rather than on the slowly descending portion shown in Ref. 17.

Lift, the component of the aerodynamic force perpendicular to the relative wind velocity, is given by

$$\mathbf{L}=-\frac{\rho C_L A \mathbf{V}_r\cdot\mathbf{V}_r}{2}\,\frac{\mathbf{V}_r\times\omega_b\mathbf{n}_2}{|\mathbf{V}_r\times\omega_b\mathbf{n}_2|}. \tag{28}$$

The lift coefficient, C_L, is only a weak function of Re, but depends on the orientation of the seams (two and four seam pitches are defined by the number of seams that trip the boundary layer at the ball's surface during each rotation). In addition, C_L strongly depends on the spin parameter $S=r_b\omega_b/|\mathbf{V}_r|$ (see Fig. 4). The lift coefficient used in the flight simulation is marked by a line and is a bilinear best fit to all C_L vs S data from previous work of Watts and Ferrer,[6] Alaways and Hubbard[8] and unpublished work of Sikorsky and Lightfoot,[8]

$$\begin{aligned} C_L&=1.5S, \quad S\leqslant 0.1,\\ C_L&=0.09+0.6S, \quad S>0.1. \end{aligned} \tag{29}$$

This approximation ignores the effect of seam orientation that is present only at low spin.

Shear stresses on the spinning ball surface cause a torque about the center of mass. It was estimated that the spin decays by only about 1.5% over a typical 5 s flight when $\omega=800$ rad/s.[7] Recent experimental research[21,22] on golf balls has measured spin decay characteristic times of about 16 s. When these results are extended to the case of baseball, they predict characteristic times of between 30 and 50 s, and result in slightly larger (10%–15%) spin decay in a typical flight. Because of the decreasing slope of the C_L-S curve, however, this longer decay time would result in only a 6%–10% change in the lift coefficient, and this only at the end of the flight. For these reasons we have neglected the decay of the spin entirely and assume as in Ref. 7 that spin is constant throughout the flight.

Note that the spin decay time constant and the functional dependencies of the drag and lift forces on Re and spin parameter are among the least well understood parts of the model. Further research is needed to provide a more detailed understanding of these relationships, but the dependencies that we have assumed are our best estimates at present.

State equations were numerically integrated (using MATLAB[23] function *ode15s* for stiff systems) to determine the ball flight trajectory with the forces due to gravity, drag, and lift included. The velocity and angular velocity initial conditions were obtained at separation from impact. The initial ball height was taken to be $y(0)=1$ m. The range was determined by interpolating to finding the horizontal distance $x(t_f)$ at the time t_f when the ball strikes the ground, $y(t_f)=0$.

E. Batting for maximum range

The batting problem consists of two phases; impact and flight. Each phase can be simulated using MATLAB input–output functions, and the phases can be linked because the final conditions on the ball from the impact serve as initial conditions for the flight. The modular nature of the problem is convenient because it allows the phases to be studied sepa-

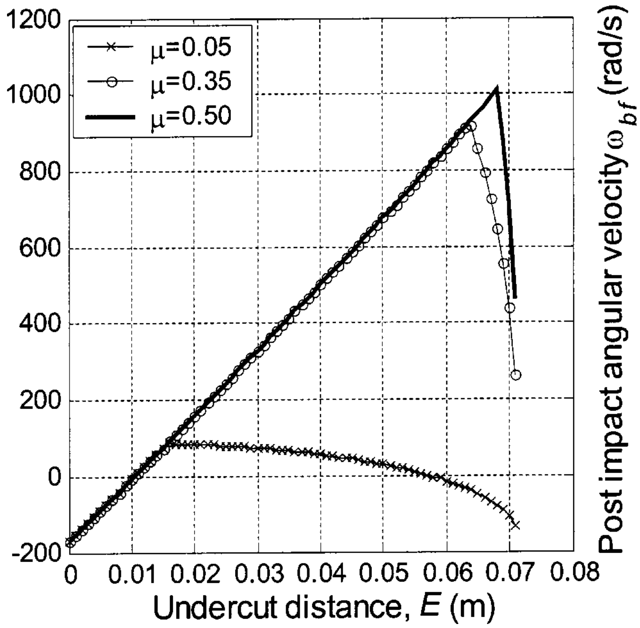

Fig. 5. Post-impact ball angular velocity ω_{bf} vs undercut distance E. For reasonably large coefficients of friction $0.35<\mu<0.5$, the same spin is achieved for all fairly hit balls ($\zeta<\pi/2$).

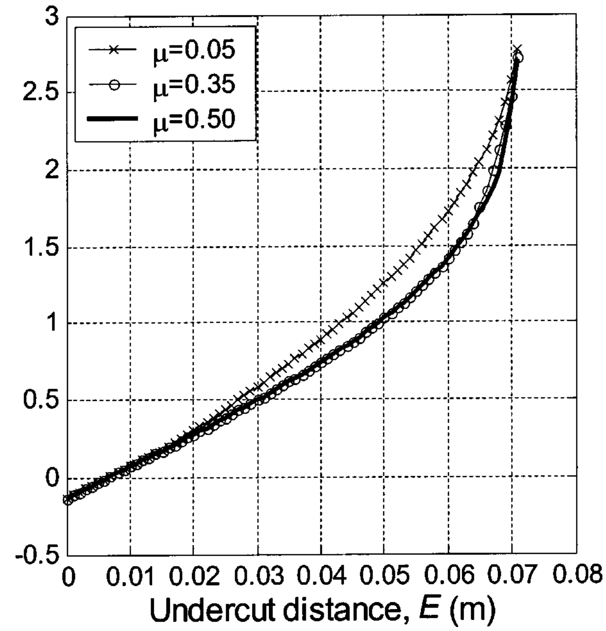

Fig. 6. Post-impact launch angle ζ vs undercut distance E. For reasonably large coefficients of friction $0.35<\mu<0.5$, the same launch angle is achieved for all fairly hit balls ($\zeta<\pi/2$).

rately and in sequence with a single simulation that takes impact initial conditions and outputs the range of the batted ball.

Furthermore, the problem can be posed as one of optimal control. The objective of the optimization is to maximize the range of the batted ball subject to variables over which the batter has control and that have optimum values that are independent of the constraints of the model. The control variables are the undercut distance E and the bat swing angle ψ. The initial conditions $(V_{b0}, V_{B0}, \omega_{b0}, \omega_{B0}, V_w)$ are not optimizable; that is, the optimization would either increase or decrease them without bound to achieve maximum range. The MATLAB function *fminsearch*[23] was used to find the optimum control variables by minimizing the negative range (maximizing positive range) with the Nelder–Mead simplex direct search method tolerances set to 0.0001.

III. RESULTS AND DISCUSSION

By using Eq. (24), the static coefficient of friction μ between a new ball and new bats of wood and aluminum was measured to be 0.50 ± 0.04 and 0.35 ± 0.03, respectively. Although μ will probably change with wear and, in the case of wood bats, may be more a function of the surface finish than the underlying material, these values are markedly larger than even the largest value considered in Ref. 7. This more realistic value of the coefficient of friction has substantial implications for the backspin a batter is able to achieve and the undercut required to produce it.

The impact simulation was used alone to study the effects of undercut distance and bat swing angle on batted ball spin and launch angle. In Figs. 5 and 6 ω_{bf} and ζ are shown as a function of the undercut distance E for $\psi=0$. Figure 5 shows the post-impact ball angular velocity as a function of E for three values of $\mu=0.05$, 0.35, and 0.50, and for an initial ball spin of $\omega_{b0}=-200$ rad/s. Other conditions held constant were $\hat{V}_{b0}=38$ m/s, $\hat{V}_{B0}=32$ m/s (as in Ref. 7) and $\psi=0$. A realistic vertical component of the ball velocity prior to impact was calculated from Eq. (3), $\hat{V}_{by0}=-5.7$ m/s, unlike the assumption in Fig. 2 of Ref. 7 that $\hat{V}_{by0}=0$. This difference in vertical velocities shifts the curves to the right about 3 mm, but otherwise causes little change.

For a given value of μ, the batted ball backspin increases as the undercut distance E increases, but at a rate only about 1/3 that predicted by Fig. 2 of Ref. 7. Although the curves of Watts and Baroni[7] are similar, there appears to be a numerical error in their results. For small E, slip halts during the collision, and at a critical value of E, a cusp in the curve corresponds to the undercut at which slip halts exactly at the moment of separation. Slip is maintained throughout impact for larger E.

For even the smallest realistic value of $\mu=0.35$ (aluminum), the slip halts during impact for undercuts less than $E=0.64$, in other words, for almost all batted balls (even foul balls). A batted backspin of 1000 rad/s can be achieved for a pitched fastball, but this requires an undercut of $E=0.068$ m rather than the 0.025 that would be extrapolated from Fig. 2 of Ref. 7. The effects of finite deformation on the change in the spin during impact are likely to increase the ratio of the impulse for sliding to the impulse for compression p_s/p_f, because the greater deformation of the ball slightly increases the moment of inertia and reduces the radial distance between the center-of-mass and the contact point. Nevertheless, in almost all cases slip halts before separation so that the modest finite deformation occurring during batting does not significantly alter the calculated changes in spin.

Predictions of post-impact launch angle (Fig. 6) are significantly affected by the value of the coefficient of friction. If we use realistic values of μ and an undercut $E=0.040$ m, we obtain a launch angle $\zeta=0.731$ rad, considerably (8.6°) less than the value of $\zeta=0.881$ rad for $\mu=0.05$.

Table II. Optimum control variables and maximum range for typical pitches. Slower curve balls with pitched topspin can be batted farther than fastballs with backspin because batted speed and launch angle need not be sacrificed for spin.

Pitch type	$\hat{V}_{b0}$ (m/s)	$\hat{V}_{B0}$ (m/s)	ω_{b0} (rad/s)	$\hat{V}_{bf}$ (m/s)	ω_{bf} (rad/s)	ζ (rad)	E_{opt} (m)	ψ_{opt} (rad)	Optimal range (m)
Fast	42.00	30.00	−200.00	44.30	191.35	0.4600	0.0265	0.1594	134.798
Knuckle	36.00	30.00	0.00	44.04	226.87	0.4499	0.0250	0.1549	135.771
Curve	35.00	30.00	200.00	43.04	276.78	0.4245	0.0223	0.1152	138.831

However, with both wooden and aluminum bats, the same launch angle is achieved up to $E=0.064\,\text{m}$, so that the differences between the two are unimportant.

Figures 5 and 6 show that, although it is important to use realistic values of μ, the 0.15 difference between μ for aluminum and wood makes no appreciable difference in batting. As long as the friction is large enough to halt slip during the collision, any additional friction does not help. For all balls hit into the field of play, wood and aluminum bats behave identically with regard to the effect of friction because slip does halt during impact. This is because, in batting, the initial ratio of tangential to normal velocities of the contact point is so small. Adair[17] (p. 77) has made essentially this point in a less technical way without resort to the concept of ''coefficient of friction,'' noting that it is probably futile to modify the bat in an attempt to increase the friction between it and the ball.

Combining the impact and flight models, two-dimensional optimizations of range were done in $E-\psi$ space for a constant initial bat speed $\hat{V}_{B0}=30\,\text{m/s}$ and no initial bat angular velocity ($\omega_{B0}=0$ rad/s) for the fastball parameter set (Table II) and no wind. Shown in Fig. 7 are contours of constant range for a fastball. The optimum range of 134.80 m (442 ft) occurs at $E=0.0265\,\text{m}$ and bat swing angle $\psi=0.159$ rad (9°), shown as point O in Fig. 7. The optimum is more sensitive to variations in E than to those in ψ, but there is little correlation between the two. To obtain a range greater than 120 m, it is necessary to maintain an undercut in the relatively narrow range $0.020<E<0.036\,\text{m}$ while still choosing ψ correctly, whereas this range can be obtained with the correct value of E over a much wider range in bat swing angle of roughly $-0.3<\psi<0.7$ rad. Thus optimal hitting is much more sensitive to bat placement than to the direction of the bat velocity at contact.

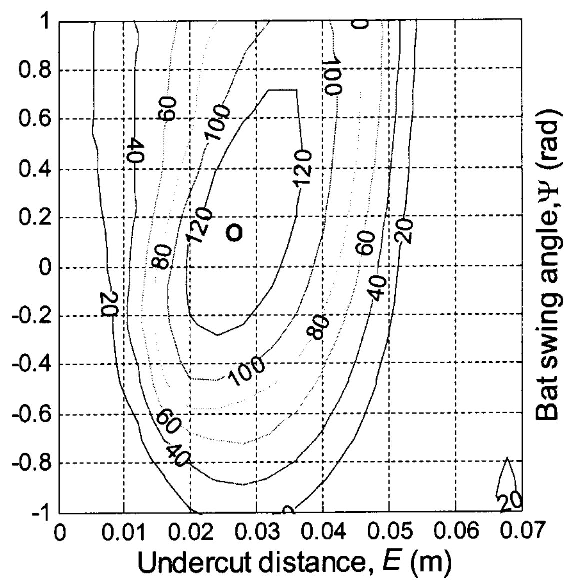

Fig. 7. Fastball range contours in control parameter space (E,ψ). The maximum range is less sensitive to changes in the bat swing angle ψ than the undercut distance E.

Optimal values $(E_{\text{opt}},\psi_{\text{opt}})$ for the undercut and bat swing angle that result in maximum range were computed for a fastball, curve ball, and knuckleball. The results are reported in Table II with the assumed characteristics of each pitch type and post-impact ball speed, rotation rate, and launch angle (initial flight conditions). Optimizations for different types of pitch (knuckleball and curve ball, Table II) yielded similar shaped contours with optima only slightly displaced from that of the fastball in Fig. 7. Table II shows clearly that, as the spin on the pitch changes from backspin (fastball) to topspin (curve ball), the amount of undercut required for maximum range decreases, but only by about 4 mm, which was first noted in Ref. 7. In addition, the optimum bat swing angle ψ decreases slightly from 0.1594 to 0.1152 rad.

Perhaps the most surprising result in Table II is that the range of the optimally batted curve ball is *larger* than that of the optimally hit fastball. It is widely held (see, for example, Ref. 17, p. 93) that ''For a given bat speed, a solidly hit fastball goes farther than a well-hit slow curve.'' This belief is not true due to the overwhelming importance of spin on range. Note that the batted ball speed of the fastball is slightly (1.26 m/s) higher than that of the curve ball, due mainly to the larger pitch speed. But the batted backspin (191 rad/s) for the fastball is 30% smaller than that of the curve ball because the pitched fastball has backspin that must be reversed during batting, whereas the curve ball has initial topspin that is augmented. This larger backspin for the curve ball increases the optimal range by 4.0 m. Finally, note that the launch angles of the optimally batted balls decrease minimally from 0.4600 to 0.4245 rad (26.3° to 24.3°) as the pitched spin changes from backspin to topspin. This effect also has been noted in Ref. 7. These launch angles are considerably less than the roughly 35° previously thought to be needed to clear the outfield fence (Ref. 17, p. 97).

It is important to be clear about the assumptions and their effects on the results. For this reason we have done comprehensive sensitivity studies of many of the parameters. In each case the parameters were varied and the optimal behavior calculated, holding other parameters constant at their values for a fastball.

Another of the variables that is not well known is bat speed, because it has infrequently been measured. Although our bat velocity of 30 m/s is representative of the ''sweet spot'' velocity for major league hitters, a bat speed of $V_{B0}=26\,\text{m/s}$ has been measured for ''average'' college hitters by Fleisig *et al.*[24] Welch *et al.*[25] measured a maximum linear bat velocity of 31 m/s. Figure 8 shows that the optimal range is

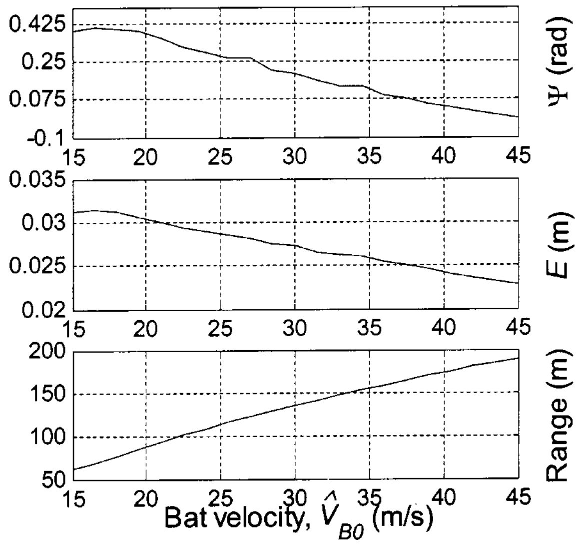

Fig. 8. Sensitivity of the fastball optimum range and control variables to bat velocity, the most important batting factor.

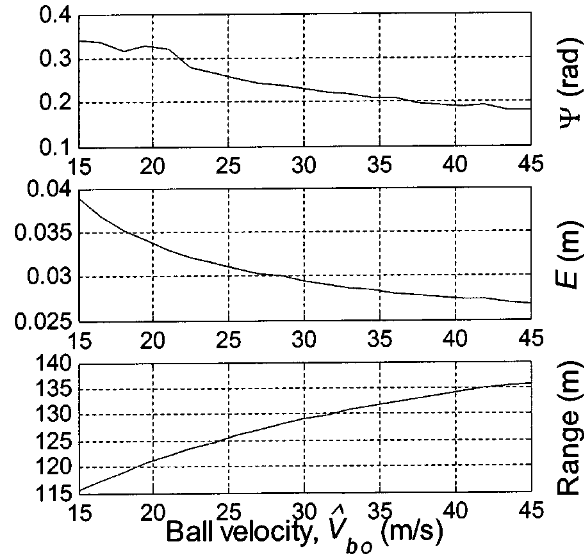

Fig. 10. Sensitivity of the fastball optimum range and control variables to pitched ball velocity.

enormously sensitive to this variable. Increasing the bat speed by only 1 m/s increases the optimal range by nearly 5 m. And although the optimum undercut varies by only a few millimeters over the entire range of bat speeds considered, the best bat swing angle decreases until a level swing is optimal at a bat speed of 42 m/s. Above this speed it is optimal to swing down on the ball.

Some batting manuals teach that rolling the wrists during the swing can increase batting performance. Figure 9 shows that this effect is minimal. A bat angular velocity of 50 or 60 rad/s is the largest conceivable roll rate, but this roll rate achieves only a modest increase of 1.8 m in the optimal range. Almost certainly, the penalties paid for this unnatural motion would be significantly greater than the benefits gained.

Even though we have above retired the myth that fastballs can be hit farther than curve balls, Fig. 10 shows that a faster fastball can indeed be hit farther than a slower one. Slower fastballs should be hit with more undercut and larger ψ. Although it is possible to hit a curve farther than other pitch types, it is probably more difficult to achieve the optimal hitting conditions for a curve ball because its pitched trajectory has a substantially larger curvature.

Figure 11 reinforces the point made earlier that a ball with topspin can be hit farther than one without. The maximum range increases with pitched topspin, if pitch velocity and bat velocity are held constant. Figure 11 also demonstrates that as pitched topspin increases, both the optimal undercut and bat swing angle decrease. A comparison of Figs. 10 and 11 shows that the possible increase in range of about 8 m due to pitched ball spin changes alone (which can certainly vary between $-200<\omega_{b0}<200$ rad/s) outweighs that of about 3 m due to pitched ball speed variations alone ($35<V_{b0}<45$ m/s).

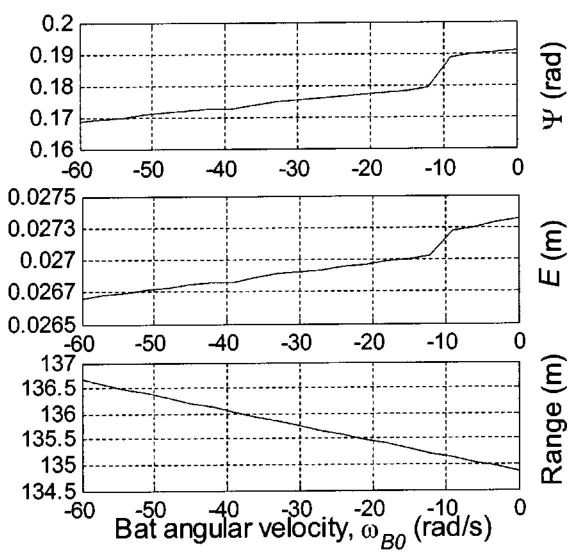

Fig. 9. Sensitivity of the fastball optimum range and control variables to bat angular velocity. Pre-impact bat spin affects range only minimally and probably should not be used in a batting strategy to increase range.

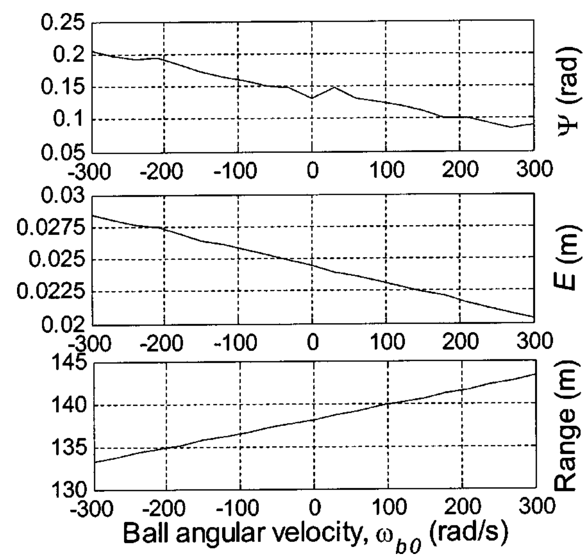

Fig. 11. Sensitivity of the fastball optimum range and control variables to pitched ball angular velocity. At the same pitch speed, pitched ball topspin increases batted ball backspin and consequently lift (Fig. 4) and increases range substantially.

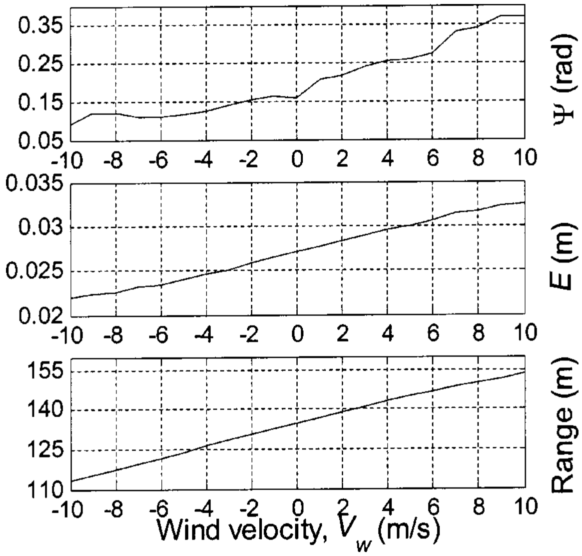

Fig. 12. Sensitivity of the fastball optimum batted range and control variables to wind velocity. Head winds from the outfield correspond to $V_w < 0$.

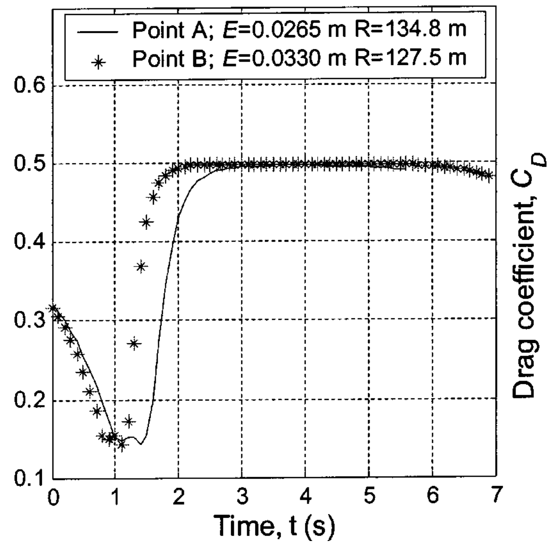

Fig. 14. C_D vs time in flight for the trajectories corresponding to both points *A* and *B* in Fig. 13. The high sensitivity of range to undercut distance can be partially attributed to the effects of the drag crisis.

In all of the sensitivity studies note that the ψ_{opt} figures are uniformly the least smooth, indicating that the optimization calculations are probably least accurate in this variable. This is to be expected because, as previously noted, the ridge of the range contours is longest and flattest in the ψ direction, contributing to the difficulty of achieving accurate results in this direction.

Figure 12 illustrates the sensitivity of optimal range to pure headwinds ($V_w < 0$) and tailwinds. As expected, with a tailwind the optimal strategy is to uppercut more and thereby increase the flight time during which the effects of the wind can be active.

The sensitivity of the optimal range to undercut is illustrated in Fig. 13, which is a slice of the optimal range surface at $\psi = 0.1594$ (the optimum value for a fastball). The two points labeled *A* and *B* differ only in undercut by 6.5 mm and their ranges differ by 7.3 m. Shown in Fig. 14 is a plot of the drag coefficients on the two trajectories as functions of time.

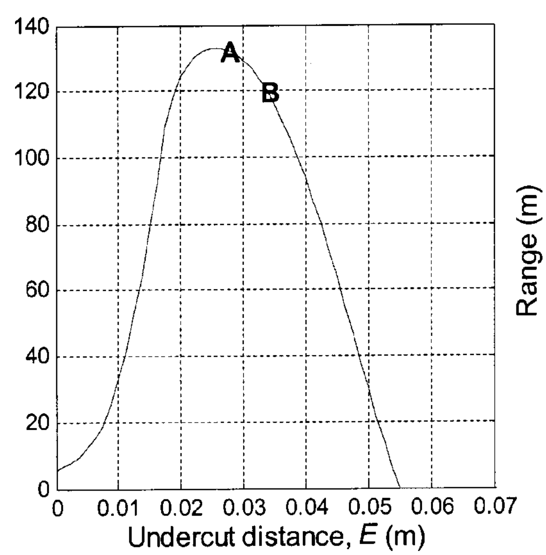

Fig. 13. Fastball range vs the undercut distance at $\psi = 0.1594$. Points *A* and *B* differ in undercut distance by 6.5 mm and in range by 7.3 m.

The initial conditions of points *A* ($\hat{V}_{bf} = 44.34$ m/s, $\omega_{bf} = 182.4$ rad/s, and $\zeta = 0.448$ rad) and *B* ($\hat{V}_{bf} = 43.63$ m/s, $\omega_{bf} = 308.3$ rad/s, and $\zeta = 0.615$ rad) differ substantially in batted ball spin and in launch angle. In spite of these differences, both trajectories pass through the drag crisis slowing during the ascent and lose enough energy to drag so that they remain below the drag crisis during the descent. The main effect on the range appears to be the increased time spent at high drag by trajectory B.

IV. CONCLUSIONS

The aim of this study was to establish an optimum strategy for hitting a baseball. The results we have presented show the following.

(1) It is important to utilize impact and flight models that are as realistic and complete as possible. Without accurate simulations, optimization is pointless. Our flight model includes the experimental lift and drag coefficient dependence on Re and spin parameter. The impact model treats collision relative velocity as a function of impulse and incorporates the dependence of the energetic coefficient of restitution e_* on the impact relative velocity and the dependence of the pitched ball angle with the horizontal, γ, on pitch speed.

(2) The bat–ball coefficient of friction μ is near 0.50 for wooden bats and 0.35 for aluminum bats.

(3) Within a realistic range (0.35–0.50), the value of μ does not affect batted ball spin, velocity, or launch angle. Therefore, any effort to increase backspin on the batted ball by increasing μ is futile.

(4) The batted ball clearly goes through the drag crisis. The resulting sharp reduction in drag leads to ranges considerably larger than would be achieved with a perfectly smooth ball which would experience drag coefficients near $C_D = 0.5$ for much, if not all, of its flight.

(5) There is an optimal strategy for achieving maximum range. For a typical fastball the batter should undercut the ball by 2.65 cm and swing upward at an angle 0.1594 rad.

(6) The optimally hit curve ball will travel farther than both the fastball and knuckleball, because of beneficial topspin on the pitched curve ball that is enhanced during impact with the bat.
(7) Range is most sensitive to bat speed, which suggests that a batter ought to work on bat speed before anything else to increase the range of his/her hits.
(8) Range is not very sensitive to wrist roll. Attempts to roll the wrists on impact do not increase range enough for it to be a useful and advantageous strategy. Wrist roll may actually limit bat speed, which is clearly more important.
(9) For a given pitch type, range increases with pitch speed.

ACKNOWLEDGMENTS

This paper is dedicated to Phil Swimley, the recently retired UC Davis head baseball coach whose teams tallied more than 900 wins during his career, and whose several stimulating discussions helped sharpen the research questions. Coaches Matt Vaughn and Ralph Rago helped in other ways. We also gratefully acknowledge the assistance of Alan Nathan (who read an early version of the manuscript and suggested that we include the analytical expression for the equivalent bat mass), James Sherwood, and Big 5 Sports in Davis, CA, on whose floor the coefficient of friction experiments were conducted.

[a]Author to whom correspondence should be addressed; electronic mail: mhubbard@ucdavis.edu

[1]L. J. Briggs, "Effect of spin and speed on the lateral deflection (curve) of a baseball; and the Magnus effect for smooth spheres," Am. J. Phys. **27**, 589–596 (1959).
[2]E. Achenbach, "The effects of surface roughness and tunnel blockage on the flow past spheres," J. Fluid Mech. **65** (1), 113–125 (1974).
[3]R. G. Watts and E. Sawyer, "Aerodynamics of a knuckleball," Am. J. Phys. **43** (11), 960–963 (1975).
[4]C. Frohlich, "Aerodynamic drag crisis and its possible effect on the flight of baseballs," Am. J. Phys. **52** (4), 325–334 (1984).
[5]A. F. Rex, "The effect of spin on the flight of batted baseballs," Am. J. Phys. **53** (11), 1073–1075 (1985).
[6]R. G. Watts and R. Ferrer, "The lateral force on a spinning sphere: Aerodynamics of a curve ball," Am. J. Phys. **55** (1), 40–44 (1987).
[7]R. G. Watts and S. Baroni, "Baseball-bat collisions and the resulting trajectories of spinning balls," Am. J. Phys. **57** (1), 40–45 (1989).
[8]L. W. Alaways, S. P. Mish, and M. Hubbard, "Identification of release conditions and aerodynamic forces in pitched-baseball trajectories," J. Appl. Biomech. **17** (1), 63–76 (2001).
[9]L. W. Alaways and M. Hubbard, "Experimental determination of baseball spin and lift," J. Sports Sci. **19**, 349–358 (2001).
[10]P. Kirkpatrick, "Batting the ball," Am. J. Phys. **31**, 606 (1963).
[11]D. T. Kagan, "The effects of coefficient of restitution variations on long fly balls," Am. J. Phys. **58** (2), 151–154 (1990).
[12]H. Brody, "Models of baseball bats," Am. J. Phys. **58** (8), 756–758 (1990).
[13]L. L. Van Zandt, "The dynamic theory of the baseball bat," Am. J. Phys. **60** (2), 172–181 (1992).
[14]R. Cross, "The sweet spot of a baseball bat," Am. J. Phys. **66** (9), 772–779 (1998).
[15]R. Cross, "Impact of a ball with a bat or racket," Am. J. Phys. **67** (8), 692–702 (1999).
[16]A. M. Nathan, "Dynamics of the baseball-bat collision," Am. J. Phys. **68** (11), 979–990 (2000).
[17]R. K. Adair, *The Physics of Baseball* (HarperCollins, New York, 2002), 3rd ed.
[18]W. J. Stronge, *Impact Mechanics* (Cambridge U.P., Cambridge, UK, 2000).
[19]S. P. Hendee, R. M. Greenwald, and J. J. Crisco, "Static and dynamic properties of various baseballs," J. Appl. Biomech. **14** (4), 390–400 (1998).
[20]R. D. Mehta and J. M. Pallis, "Sports ball aerodynamics: Effects of velocity, spin and surface roughness," in *Materials and Science in Sports*, edited by F. H. Froes and S. J. Haake (TMS, Warrendale, PA, 2001), pp. 185–197.
[21]A. J. Smits and D. R. Smith, "A new aerodynamic model of a golf ball in flight," in *Science and Golf II*, Proceedings of the 1994 World Scientific Congress of Golf, edited by A. J. Cochran and M. R. Farrally (E&FN Spon, London), pp. 340–347.
[22]G. Tavares, K. Shannon, and T. Melvin, "Golf ball spin decay model based on radar measurements," in *Science and Golf III*, Proceedings of the 1998 World Scientific Congress of Golf, edited by M. R. Farrally and A. J. Cochran (Human Kinetics, Champaign, IL, 1999), pp. 464–472.
[23]D. Hanselman and B. Littlefield, *Mastering MATLAB 6: A Comprehensive Tutorial and Reference* (Prentice–Hall, Upper Saddle River, NJ, 2001).
[24]G. S. Fleisig, N. Zheng, D. F. Stodden, and J. R. Andrews, "Relationship between bat mass properties and bat velocity," Sports Eng. **5**, 1–8 (2002).
[25]C. M. Welch, S. A. Banks, F. F. Cook, and P. Draovitch, "Hitting a baseball: A biomechanical description," J. Orthop. Sports Phys. Ther. **22** (5), 193–201 (1995).

A VIEW OF EINSTEIN

Nevertheless, the loftiness of his thought, as over against the brutality of the times and of its applications, was such that even the public obscurely sensed in him the symbol of the cultural predicament of physics: in the sad, sweet face; in that simplicity more suited to some other civilization, some gentler world; in the strange, the often inappropriate moments chosen for speech; in the great, the profound, the somehow altogether impersonal benevolence; in what shames the spotted adult as the innocence of a wise child.

C. Gillispie, *The Edge of Objectivity* (Princeton University Press, 1960), p. 519.
Submitted by Gary E. Bowman.